Multiphoton Infrared Laser-Induced Absorption and Reaction of Organic Esters

Wayne C. Danen,* V. C. Rio, and D. W. Setser

Contribution from the Department of Chemistry, Kansas State University, Manhattan, Kansas 66506. *Received April 16, 1981*

Abstract: Date are reported for the multiphoton, pulsed, infrared laser-induced unimolecular reactions of a series of organic esters. The dependence of the reaction probability and absorption cross sections on the laser fluence, laser frequency, reactant pressure, and bath gas pressure was determined for ethyl acetate, ethyl fluoroacetate, ethyl acrylate, *n*-butyl acetate, *sec*-butyl acetate, and ethyl 2-bromopropionate. The extent of collisional energy transfer from excited ester molecules to cold molecules was characterized by a thermal monitor molecule; collisional energy transfer leading to reaction of the monitor was negligible at pressures <0.10 torr. The laser absorption cross sections were independent of pressure but mildly dependent on fluence; all cross sections extrapolated to the single-photon, broad-band cross section at low laser fluence. Direct and sensitized excitation of the bifunctional esters (*sec*-butyl acetate and ethyl 2-bromopropionate) gave similar results, demonstrating that the absorbed laser energy was randomized before chemical reaction. Log–log plots of reaction probability, $P(\phi)$, vs. fluence showed approximately linear behavior for $P(\phi) = 10^{-2}$–10^{-4} with slopes of 4–6. At high fluences $P(\phi)$ values asymptotically approach constant values between 0.6 and 1.0. For ethyl acetate and ethyl fluoroacetate the reaction probability for the same amount of absorbed energy was dependent on laser frequency and fluence; this is evidence that only a certain, fluence-dependent, fraction of molecules absorb the laser energy. Addition of bath gas reduced the reaction probabilities, especially at low laser fluence, indicating that postpulse reaction was very important for $P(\phi) < 0.1$.

Introduction

Excitation in the gas phase with intense, pulsed, infrared laser radiation has been shown to promote molecules to high vibrational levels of the ground electronic state as the result of absorbing many infrared photons. Much work has been reported on relatively small molecules; SF_6 has received the most attention and may be considered the prototype for infrared laser photochemistry/photophysics. A number of recent review articles covering various aspects of this field are available.[1-7]

In contrast to the majority of the reported studies, we have centered our investigations on relatively large organic compounds.[1] We consider large molecules to be those with ≳five to six atoms other than hydrogen and possessing low-frequency modes. More specifically, a large molecule is one with a density of vibrational/rotational states in the 10^3–10^4-cm^{-1} range following absorption of one photon by a room-temperature sample. The distinction between large and small molecules is significant because of the importance of density of states for multiphoton absorption and because of the small rate constants for molecules slightly above the threshold energy.

Large molecules can be expected to have the following characteristics relative to multiphoton infrared laser-induced processes: (1) the quasi-continuum may begin in the energy region populated by the 300 K Boltzmann distribution; (2) the threshold fluence for reaction is modest and the reaction probabilities are high for molecules with cross sections larger than $\sim 10^{-19}$ cm^2; (3) rotational "hole-burning" will not be of significance; (4) the reaction rate constants near the threshold energy are small, leading to extensive incubation times and significant postpulse effects; and (5) the reaction yield is very sensitive to quenching by added bath gases. Although a few results have been interpreted as showing that the vibrational excitation remains localized during and after the excitation processes,[8-11] most results, and certainly our views, are consistent with statistically intramolecular redistribution of energy prior to unimolecular chemical reaction.

Table I. Effect of Isopropyl Bromide on the Yield and Selectivity of 0.05 torr Ethyl Acetate Irradiated at 1046.85 cm^{-1} with 2.0 and 3.6 J/cm^2

i-PrBr (torr)	ϕ	reaction probability	$Y_0{}^a$ / Y	[propylene] / [ethylene]
0.00	2.0	0.16	1.0	0.00
0.03	2.0	0.10	1.6	0.0005
0.04	2.0	0.080	2.0	0.05
0.10	2.0	0.039	4.1	0.13
0.11	2.0	0.034	4.6	0.25
0.18	2.0	0.018	9.1	0.78
0.23	2.0	0.012	13.5	1.37
0.29	2.0	0.004	40.7	1.65
0.00	3.6	0.78	1.0	0.00
0.06	3.6	0.76	1.0	0.03
0.18	3.6	0.53	1.4	0.05
0.61	3.6	0.38	2.0	0.18
1.20	3.6	0.17	4.3	1.10
2.10	3.6	0.08	8.7	6.29

[a] Y_0 is reaction yield without added isopropyl bromide; Y is reduced yield at a given pressure of added isopropyl bromide.

In this paper we report quantiative studies of the dependence of reaction probability and the absorption cross sections on laser fluence, laser frequency, reactant, and bath gas pressure for a number of organic esters. In the accompanying paper[12] modeling studies utilizing a master equation formulation are presented with emphasis on relating calculated results to the experimental low-pressure-bulb results of this paper. The esters and their unimolecular elimination reactions induced by laser energy absorption are shown in reactions 1–6. These elimination reactions occur

(1) Danen, W. C.; Jang, J. C. "Laser-Induced Chemical Processes"; Steinfeld, J. I. Ed.; Plenum: New York, 1981; Chapter 2.
(2) Danen, W. C. *Opt. Eng.* **1980**, *19*, 21–28.
(3) Schulz, P. A.; Sudbo, Aa. S.; Krajnovich, D. J.; Kwok, H. S.; Shen, Y. R.; Lee, Y. T. *Annu. Rev. Phys. Chem.* **1979**, *30*, 379–409.
(4) Ronn, A. M. *Sci. Am.* **1979**, *240*, 114–128.
(5) Cantrell, C. D.; Freund, S. M.; Lyman, J. L. "Laser Handbook", Stitch, M. L., Ed.; North-Holland: Amsterdam, 1979; Vol. III.
(6) Grunwald, E.; Dever, D. F.; Keehn, P. M. "Megawatt Infrared Laser Chemistry"; Wiley: New York, 1978.
(7) Ambartzumian, R. V.; Letokhov, V. S. "Chemical and Biochemical Applications of Lasers"; Moore, C. B., Ed.; Academic Press: New York, 1977; Vol. III, pp 167–316.
(8) Kaldor, A.; Hall, R. B.; Cox, D. M.; Horsley, J. A.; Rabinowitz, P.; Kramer, G. H. *J. Am. Chem. Soc.* **1979**, *101*, 4465.
(9) Cox, D. M.; Hall, R. B.; Horsley, J. A.; Kramer, G. H.; Rabinowitz, P.; Kaldor, A. *Science* **1979**, *205*, 390.
(10) Hall, R. B.; Kaldor, A. *J. Chem. Phys.* **1979**, *70*, 4027.
(11) Brenner, D. M. *Chem. Phys. Lett.* **1978**, *57*, 357.
(12) Jang, J. C.; Setser, D. W.; Danen, W. C. *J. Amer. Chem. Soc.*, following paper in this issue.

0002-7863/82/1504-5431$01.25/0 © 1982 American Chemical Society

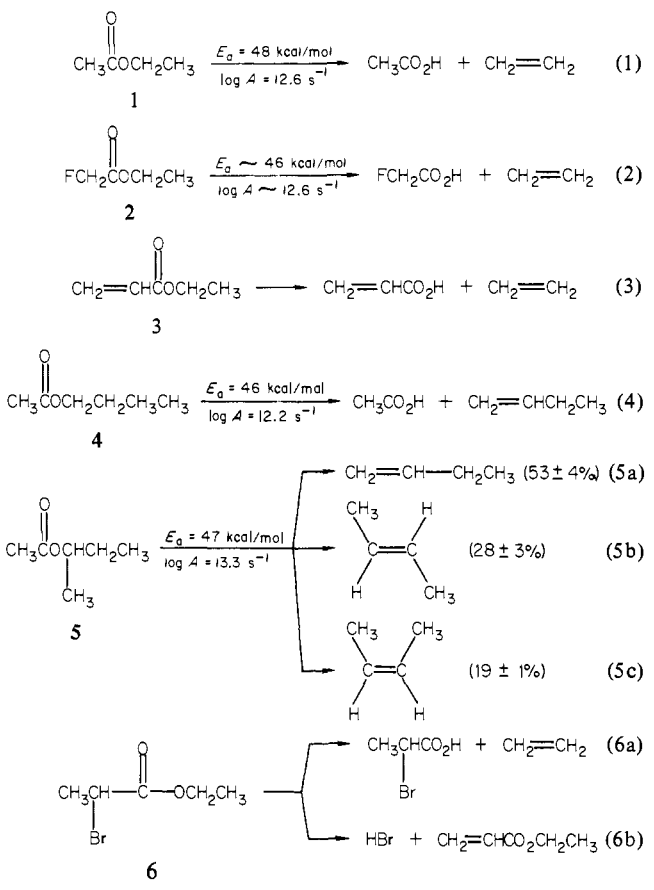

via a six-membered cyclic transition state (reaction 7) with ac-

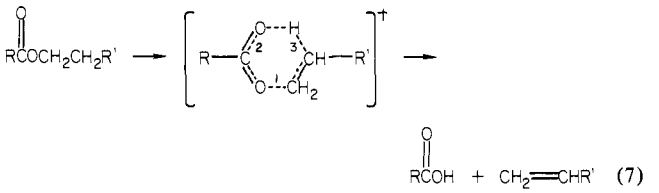

tivation energies of ~45–48 kcal/mol. The reactions are concerted but there is evidence that the extent of bond lengthening in the transition state is in the order 1 > 2 > 3[13] (see transition state depiction for reaction 7). The Arrhenius parameters for **1**,[14a] **4**,[14b] and **5**,[14c] have been determined as referenced. The parameters for **2** were estimated from the reported E_a = 43.7 kcal/mol for isopropyl fluoroacetate.[15a] (The numbers given with reaction 5 are our experimental results.)

All laser irradiations were performed under constant fluence conditions utilizing line-tuned frequencies in the 9-μ band of the CO_2 laser. Since <<5% of the laser radiation is absorbed for pressures <0.10 torr, the incident fluence, ϕ_0, is virtually the same as the transmitted fluence and there are no significant fluence gradients within the cell. Therefore, $\phi_0 \sim \phi$ (except, of course, for the relatively high-pressure absorption measurements to determine σ_L) and we will designate the laser fluence merely as ϕ.

The infrared spectrum of methyl acetate has been studied.[15b] By analogy, the strong absorption band at ~1050 cm^{-1} present in the other acetate esters can be attributed to the CH_3 rocking and stretching modes of the acid moiety. Other modes of similar frequency, but lower oscillator strength, also exist. For some esters the O-alkyl stretch mode also may contribute to the absorption. The absorption spectra for **1**–**6** are shown in Figure 1.

Experimental Section

A. CO_2 Laser. All irradiations were performed with a multimode, tunable Lumonics Model 103 TEA CO_2 laser utilizing uniform fluences of 0.2–10 J/cm^2. Attenuation of the laser energy was accomplished using varying thicknesses of Saran (copolymer of vinyl chloride and 1,1-dichloroethylene). An aperture was used to reduce the beam size and to provide a more homogeneous beam. The laser beam profile from a 20-mm aperture was measured using a 3-mm iris placed before a pyroelectric detector. The variation in fluence across the 20-mm beam was <5%. Beam diameters were determined utilizing heat-sensitive paper.

Focusing was achieved with a 50-cm focal length BaF_2 lens (Unique Optical Co.) and short sample cell which was positioned at various distances between the lens and the focal point to vary the effective fluence within the cell. Alternatively, in later studies, a Galilean telescope consisting of a 75-cm BaF_2 converging (positive focusing) lens positioned 37.5 cm in front of a 37.5-cm BaF_2 diverging (negative focusing) lens was utilized to achieve higher uniform fluence. This effectively produced a collimated laser beam 4× more intense than the incident beam and could be used with longer reaction cells. Most studies were conducted using a CO_2–He–N_2 laser gas mix which produced an initial ~130-ns fwhm pulse followed by a long tail extending to ~1.2 μs. Approximately half the energy was contained within the initial spike and half within the tail. Removing the N_2 from the gas mix eliminated the tail and gave a ~110-ns fwhm pulse. Pulse energies were measured with a Scientech Model 38-0102 volume absorbing disk calorimeter or a Lumonics Model 20D pyroelectric detector. The pulse temporal profile was measured with a Rofin photon drag detector. The laser lines were identified with an Optical Engineering, Inc. Model 16-A CO_2 laser spectrum analyzer.

B. Irradiation Cells. Samples for laser irradiation were prepared by standard vacuum-line techniques. The cells were made from Pyrex tubing equipped with Teflon/Viton O-ring valves and fitted with NaCl windows. Gas pressures were monitored with a MKS Baratron Type 222AHS-A-B-10 pressure transducer. The cells varied from 2.0 to 4.0 cm in diameter and 0.95 to 100 cm in length. The 0.95-cm length cell was utilized when high fluences were obtained with the 50-cm focal length BaF_2 lens to preclude fluence gradients along the irradiated volume. Thus, all irradiations were performed with constant fluence throughout the irradiated volume.

C. Absorption Measurements. The absorbed energy per laser pulse was measured with a pair of pyroelectric detectors (Lumonics Model 20D) arranged as depicted in Figure 2. The signals for detectors 1 and 2 were amplified by PREAMP 1 and PREAMP 2 with adjustable gains α and β, respectively, and transmitted to a PDP/8E computer. A small (~3–4%) fraction, F_r^{NaCl}, of the laser energy, E_0, was reflected by a NaCl flat into detector 1. The remainder passed through the reaction cell and a fraction $F_r^{Ge}(1 - F_r^{NaCl})$ of the transmitted beam was reflected by a germanium flat to detector 2. A measurement first was made with the empty cell to account for window losses. The amplified signals are proportional to $\alpha F_r^{NaCl} E_0'$ for peak 1 and $\beta F_r^{Ge}(1 - F_r^{NaCl}) E_0'$ for peak 2. When the measurement was repeated with a sample in the cell and with α and β unchanged, the energy observed by the second detector was lowered by the energy deposited in the cell. This can be written as $\beta F_r^{Ge}(1 - F_r^{NaCl})(E_0\phi/\phi_0)$, where ϕ_0 and ϕ are the incident and transmitted fluences, respectively. The transmittance for a given sample pressure was obtained by dividing the ratio of signal 2 to signal 1 when the cell contained sample, by the ratio of signal 2 to signal 1 when the cell was empty (eq 8). It is important to note that α and β are not

$$\text{transmittance} = \frac{\phi}{\phi_0} = \frac{[\beta F_r^{Ge}(1 - F_r^{NaCl}) E_0 \phi/\phi_0/\alpha F_r^{NaCl} E_0]_{\text{sample}}}{[\beta F_r^{Ge}(1 - F_r^{NaCl}) E_0'/\alpha F_r^{NaCl} E_0']_{\text{empty cell}}} \quad (8)$$

changed in the two measurements and that β includes the factor for energy loss in the empty cell. If there is significant reaction for a given ϕ, only the first pulse was used in calculation of ϕ/ϕ_0. With this detection system we could measure accurately absorption of ≥2%.

Several minor modifications to the arrangement shown in Figure 2 were also employed. Fluence attenuators could be inserted at point A for low fluence experiments or a long focal length lens or Galilean telescope arrangement could be placed at point B for higher fluence conditions. For low fluence experiments, the second beam splitter was removed and detector 2 was placed directly behind the sample cell.

Absorption cross sections were also measured by an opto-acoustic detector assembled for a B&K Instruments Inc. Model 4145 microphone cartridge fixed in a cell of 10-cm length and 4-cm diameter; the opto-acoustic signal was displayed on an oscilloscope screen. Careful checks showed that the signal was a linear function of pressure at constant

(13) Taylor, R. *J. Chem. Soc., Perkin Trans. 2* **1975**, 1025.

(14) Benson, S. W.; O'Neal, H. E. Report NSRDS-NBS 21; National Bureau of Standards: Washington, D.C., 1970: (a) p 158; (b) p 160; (c) p 170; (d) p 71; (e) p 95.

(15) (a) Chuchani, G.; Hernandez, J. A.; Yepez, M.; Alonso, H. E. *Int. J. Chem. Kinet.* **1977**, *9*, 811. The increase of 3 kcal/mol to give E_a ~46.7 kcal/mol for **2** was deduced by noting the differences in E_a for several halogenated and nonhalogenated isopropyl esters as compared to the ethyl esters. The *A* factor for **2** was assumed the same as known for **1** since there is no structural reason to expect a difference. (b) George, W. D.; Houston, T. E.; Harris, W. C. *Spectrochim. Acta, Part A* **1974**, *30*, 1035.

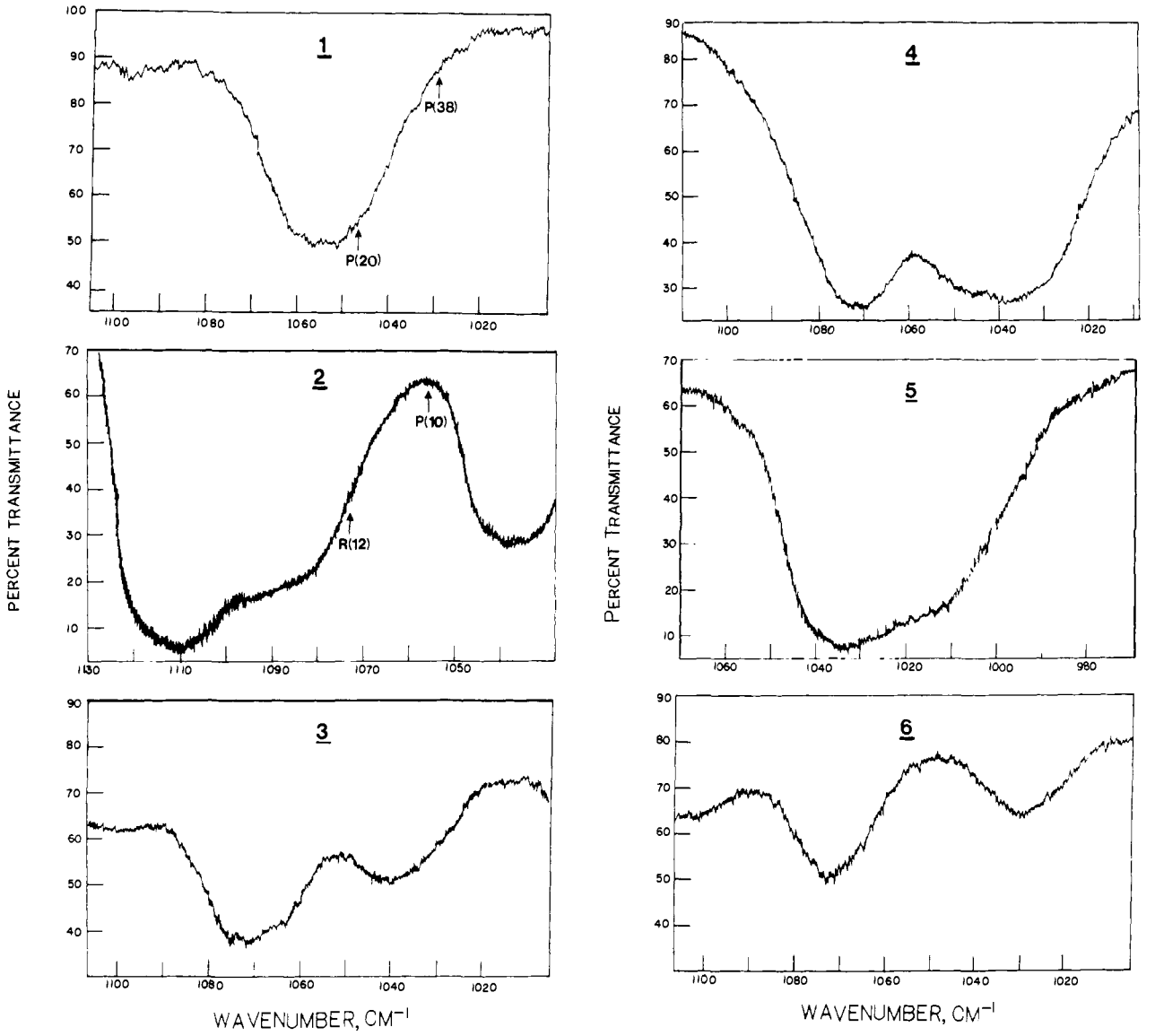

Figure 1. Gas-phase infrared spectra: **1**, 2.37 torr, 19.8 cm; **2**, 6.37 torr, 20 cm; **3**, 16.4 torr, 21 cm; **4**, 7.0 torr, 21 cm; **5**, 13.4 torr, 21 cm; **6**, 2.78 torr, 21 cm. Laser lines in the 9-μ CO_2 band utilized for **1** and **2** are noted: P(20), 1046.85 cm^{-1}; P(38), 1029.44 cm^{-1}; R(12), 1073.28 cm^{-1}; P(10), 1055.63 cm^{-1}.

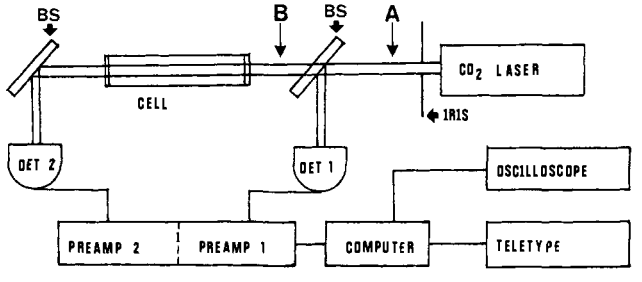

Figure 2. Experimental arrangement to measure absorbed energy per pulse. BS = beam splitter (NaCl or Ge flats); A and **B** indicate position of fluence attenuators and Galilean telescope, respectively, when utilized.

fluence and incident fluence at constant pressure. Values of σ_L at various fluences were measured by selecting one σ_L value determined by the dual detector method described above as a reference. The two methods gave similar results provided that all experiments were done at a constant pressure and a constant laser beam diameter.

D. Chemicals and Analyses. All chemicals were obtained from commercial suppliers and purified by vacuum distillation until gas–liquid chromatography (GLC) indicated no significant impurities. The reactant esters and olefinic products from the laser-induced reactions were analyzed with a Varian 2700 series gas chromatograph equipped with a flame ionization detector. A 6 ft × $^1/_8$ in. stainless steel Porapak Q column was used except for *sec*-butyl acetate, (**5**) as separation of the isomeric butene required a 30 ft × $^1/_4$ in. propylene carbonate column connected to a 5 ft × $^1/_8$ in. diameter 10% Carbowax 20M on Chromosorb W column at 0 °C. Analyses were done isothermally: 175 °C for **1**, 180 °C for **2**, 200 °C for **3** and **4**, 190 °C for **5**. Retention times for the olefins were of the order of 2 to 3 min, and those of the esters ranged from 5 to 17 min, depending on the molecular weight. Peak areas were measured using a planimeter. Absolute calibrations were made using accurately prepared samples of reactants and products.

Results

A. Thermal Monitor Studies. We define for unimolecular reactions the point at which the deposited vibrational energy has reached equilibrium among internal modes of all molecules within the irradiated volume as the differentiation point between nonequilibrium laser-induced chemistry and thermal chemistry. Complete *V*, *T*, *R* equilibration cannot be ascertained with the neat esters since vibrational excitation (only) is sufficient to drive unimolecular processes. We have described[17] a thermal monitoring technique by which the amount of laser induced reaction could be distinguished from the thermal component. The HBr elimi-

(16) Harrison, R. G.; Hawkins, H. L.; Leo, R. M., John, P. *Chem. Phys. Lett.* **1980**, *70*, 555.
(17) Danen, W. C.; Munslow, W. D.; Setser, D. W. *J. Am. Chem. Soc.* **1977**, *99*, 6961.

Table II. Effect of Varying Pressure Fluence and Laser Beam Diameter for the Irradiation of a 97:3 Mixture of Ethyl Acetate:Isopropyl Bromide

entry	pressure (torr)	fluence (J/cm²)	beam diameter (mm)	$P_{(i\text{-PrBr})}$[a]	$P_{(\text{EtOAc})}$[b]	$\frac{P_{(i\text{-PrBr})}}{P_{(\text{EtOAc})}}$[c]
1	0.05	1.35	7.5	0.00008	0.031	0.0026
2	0.05	2.49	7.5	0.0011	0.17	0.0065
3	0.20	2.49	7.5	0.056	0.19	0.29
4	0.05	1.35	19.1	0.0021	0.028	0.075

[a] Reaction probability of isoporpyl bromide monitor. [b] Reaction probability of ethyl acetate. [c] Ratio for a totally equilibrated system is ~11.

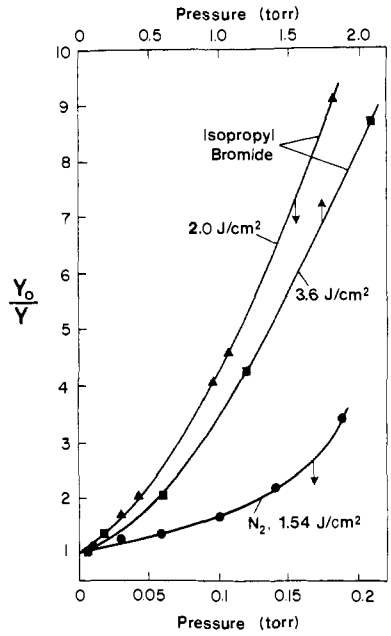

Figure 3. Stern–Volmer plot illustrating quenching effect of added isopropyl bromide and N_2 on reaction probability of 0.05 torr of ethyl acetate irradiated at 1046.85 cm^{-1} (P(20) of 9-μ band) with the indicated laser fluences. Y_0 = reaction yield per pulse without added bath gas; Y = reaction yield at indicated pressure of bath gas. Note the different pressure scales.

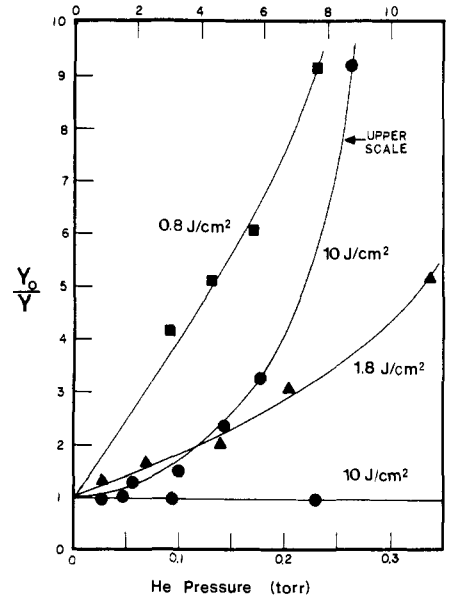

Figure 4. Stern–Volmer plot illustrating quenching effects of added He on reaction probability of 0.05 torr of ethyl acetate irradiated at 1046.85 cm^{-1} (P(20) of 9-μ band) at ϕ = 0.8, 1.8, and 10 J/cm²; Y_0 and Y as defined in Figure 3. Note the different pressure scales.

nation from isopropyl bromide was used as a thermal monitor for ethyl acetate (reaction 1) because of the similarities in activation energies ($k = 10^{12.6} \exp(-48\,000/RT)$[14a] for **1** and $k = 10^{13.6} \exp(-47\,800/RT)$[14c] for isopropyl bromide). The early work was conducted at relatively high pressures (5–60 torr) and the monitor was used to separate the laser and thermal components. However, such experiments are not the ideal way to check for a thermal rection because the addition of isopropyl bromide alters the molecular density in the irradiated volume as compared to the neat system; this can affect the amount of deposited energy, energy transfer rates, and heat capacities. Also, such a large mole fraction of thermal monitor significantly quenches the primary reaction.

Table I illustrates the quenching by isopropyl bromide of the ethyl acetate (0.05 torr) reaction yield at 1046.85 cm^{-1} (P(30) of 9-μ band) for two different laser fluences. The data are displayed in the form of a Stern–Volmer plot in Figure 3 in which Y_0 is the reaction yield without added bath gas and Y is the reduced yield at a given pressure of the added gas. Figure 3 also includes nitrogen data at 1.54 J/cm², and Figure 4 demonstrates the quenching by He at laser fluences of 0.8, 1.8, and 10 J/cm². For all of these experiments the thermal component to the reaction is negligible.

The results demonstrate that collisional deactivation of ethyl acetate is very significant even by a few tenths torr of bath gas. The addition of isopropyl bromide can lead to considerable quenching of the ethyl acetate reaction without reaction of the monitor molecule occurring. Under these conditions the isopropyl bromide realistically cannot be considered a thermal monitor, because the large mole fraction of isopropyl bromide significantly perturbed the system.

We, therefore, conducted several studies utilizing a 97:3 ethyl acetate:isopropyl bromide mixture so that the thermal monitor did not perturb the heat capacity of the system. Table II lists pertinent results; $P_{(i\text{-PrBr})}$ and $P_{(\text{EtOAc})}$ are the reaction probabilities per pulse for the monitor molecule and ethyl acetate, respectively. The first two entries show that thermal contributions are observable but of negligible importance at 0.05 torr. However, the thermal contribution increases rapidly with total pressure as illustrated by the 0.20-torr experiment. One experiment was done to check the role of the diameter of the irradiated volume, since the bulk cooling rate of the irradiated volume possibly varies inversely with the diameter. Comparing entries 1 and 4 shows that the ethyl acetate reaction probability was independent of beam diameter but that the thermal component increased with larger diameter. These geometric effects will be discussed more fully below.

Thermal monitor studies of *sec*-butyl acetate (**5**) with *tert*-butyl chloride[14d] as the monitor molecule gave results similar to those of ethyl acetate. We conclude that, for pressure ≤ 0.10 torr, thermal contribution to the yields from irradiation of the neat esters should be negligible.

B. Absorption Measurements. The transmittance as measured from eq 8 was plotted vs. sample pressure (*0.1* to *1.0* torr) for a constant-length cell. We found Beer's law behavior; the laser absorption cross section, σ_L, was determined from the slope of log ϕ/ϕ_0 vs. pressure plot by eq 9, σ_L is the absorption cross section

$$\sigma_L = \frac{2.303}{lN} \log\frac{\phi}{\phi_0} \qquad (9)$$

(cm²/molecule), l is the cell length (cm), and N was defined as the total concentration (molecules/cm³ = 3.24×10^{16} molecules/cm³·torr at room temperature). A similar, limited (σ_L is

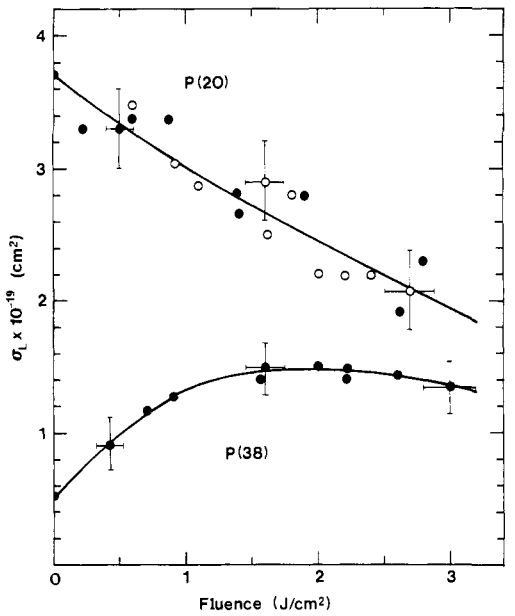

Figure 5. Effective bulk laser absorption cross section, σ_L, for ethyl acetate (**1**) vs. laser fluence for P(20) and P(38) lines of 9-μ band (1046.85 and 1029.44 cm^{-1}, respectively): ●, dual detector/computer absorption technique; O, optoacoustical detector. Estimated error limits are shown for several data points. The points at ϕ = 0 J/cm^2 were measured with a conventional (Perkin-Elmer Model 180) infrared spectrometer.

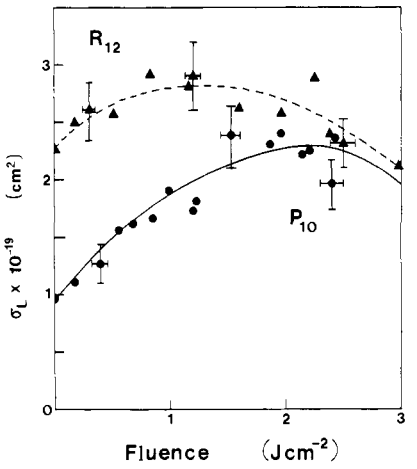

Figure 6. Effective bulk laser absorption cross section, σ_L, for ethyl fluoroacetate (**2**) vs. laser fluence for R(12) and P(10) lines of 9-μ band (1073.28 and 1055.63 cm^{-1}, respectively): ▲ R(12); ● P(10). All points were taken with dual detector/computer absorption technique. Estimated error limits are shown for several data points. The points at ϕ = 0 J/cm^2 were measured with a conventional (Perkin-Elmer Model 180) infrared spectrometer.

independent of pressure but not ϕ) Beer's law dependence has been reported for cyclobutanone;[16] small molecules frequently do not exhibit such dependence but, instead, have pressure-dependent cross sections.

Figures 5–7 illustrate the dependence of σ_L on laser fluence for esters **1–6**. Ethyl acetate (**1**) and ethyl fluoroacetate (**2**) were studied in most detail. Estimated error limits, from uncertainties in ϕ and ϕ/ϕ_0, are shown in Figures 5 and 6. At low fluence all the σ_L curves extrapolate to the single-photon, broad-band spectroscopic cross sections at the frequencies of interest, as measured at ~1 cm^{-1} resolution in our laboratory; see Figures 5–7. For the majority of the esters, σ_L changes by less than a factor of 2 even at fluences as high as 5 J/cm^2. This contrasts with the behavior of small molecules which frequently exhibit a substantial decrease in σ_L with increasing fluence. Although σ_L decreased somewhat with increasing fluence for **1** and **3–6**, σ_L

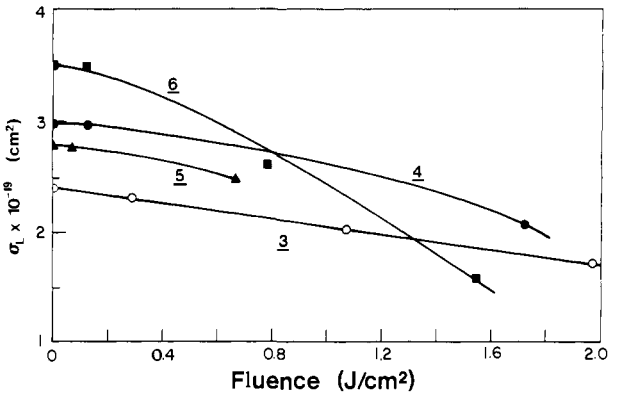

Figure 7. Effective bulk laser absorption cross sections, σ_L, vs. laser fluence for **3** at R(10) (1071.88 cm^{-1}), **4** at P(26) (1041.28 cm^{-1}), **5** at P(38) (1029.44 cm^{-1}), and **6** at R(12) (1073.28 cm^{-1}). The points at ϕ = 0 J/cm^2 were measured with a conventional (Perkin-Elmer Model 180) infrared spectrometer.

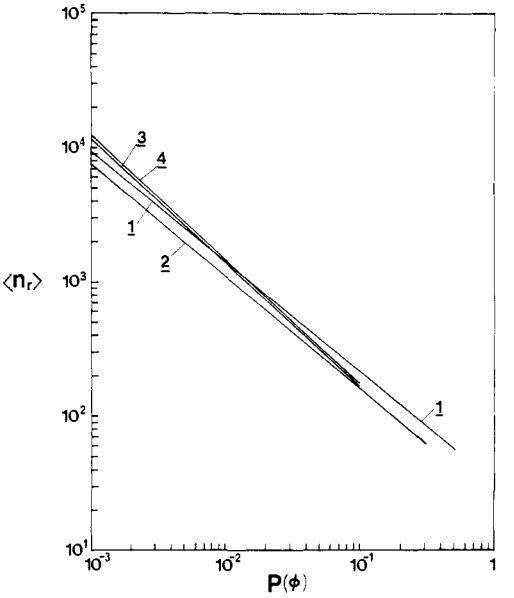

Figure 8. Average number of photons absorbed per reacted molecule, $\langle n_r \rangle$, vs. reaction probability, $P(\phi)$, for 1–**4**.

actually increased with fluence for **1** at 1029.44 cm^{-1} and **2** at both 1055.63 and 1073.28 cm^{-1}. These three frequencies all lie to the low-frequency side of the band maximum of **1** and **2**.

The average number of photons absorbed per molecule in the irradiated volume, $\langle n \rangle$, is given by eq 10. A related quantity

$$\langle n \rangle = \phi_0 \sigma_L / hc\nu \qquad (10)$$

is the average number of photons absorbed per *reacted* molecule, $\langle n_r \rangle$, which is simply $\langle n \rangle$ divided by the fraction of molecules that react in the irradiated volume per pulse, $P(\phi)$. Figure 8 depicts $\langle n_r \rangle$ vs. $P(\phi)$ for **1–4**.

To obtain the total average vibrational energy of the laser-excited molecules, the thermal room-temperature vibrational energy, $\langle E_{(\text{thermal})} \rangle$, must be added to $\langle n \rangle$. This contribution, which can be calculated by eq 11, is 3.0 kcal mol^{-1} (1.0 photon) for **1** and **2**, and 4.0 kcal mol^{-1} (1.3 photon) for **3–5**.

$$\frac{\langle E_{(\text{thermal})} \rangle}{RT} = \sum_{i=1}^{3n-6} \frac{h\nu_i/(kT)}{\exp(h\nu_i/kT) - 1} \qquad (11)$$

C. Reaction-Probability Measurements. The reaction probability at a given laser fluence, $P(\phi)$, is defined as the number of molecules in the irradiated volume that react per pulse divided by the total number of molecules in the irradiated volume. $P(\phi)$ is calculated from eq 12 in which V_T and V_{1r} refer to the total

$$P(\phi) = (V_T/V_{1r})[1 - (C_i/C_0)^{1/i}] \qquad (12)$$

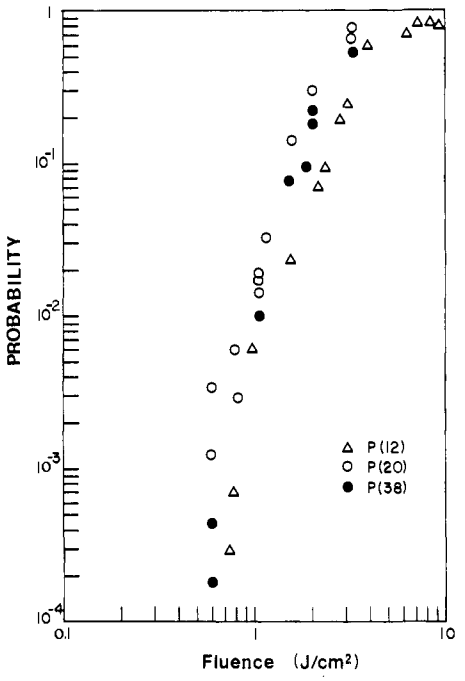

Figure 9. Reaction probability per pulse vs. laser fluence for 0.05 torr of **1** irradiated at P(12) (1053.92 cm^{-1}), P(20) (1046.85 cm^{-1}), and P(38) (1029.44 cm^{-1}).

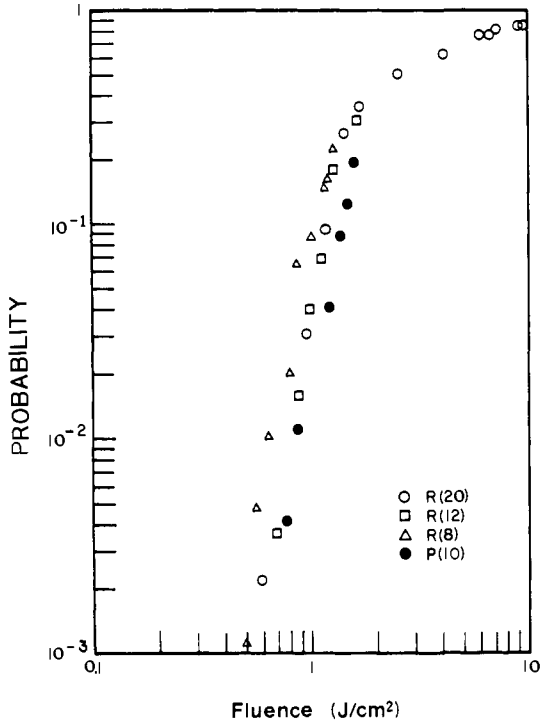

Figure 10. Reaction probability per pulse vs. laser fluence for 0.05 torr of **2** irradiated at R(20) (1078.59 cm^{-1}), R(12) (1073.28 cm^{-1}), R(8) (1070.46 cm^{-1}), and P(10) (1055.63 cm^{-1}).

cell volume and the irradiated volume, respectively. Figures 9 and 10 summarize the results on log $P(\phi)$ vs. ϕ for **1** and **2**; $P(\phi)$ is a strong function of ϕ. Figure 11 depicts the reaction probability $P(\langle n\rangle)$ of **1** and **2** vs. the average number of adsorbed photons, $\langle n\rangle$, at two different laser frequencies for each. Plots of $P(\langle n\rangle)$ vs. $\langle n\rangle$ should be inherently more informative[18] than $P(\phi)$ vs. ϕ since the extent of reaction is directly related to the absorbed energy and only indirectly (via σ_L) for ϕ.

(18) Dever, D. F.; Grunwald, E. *J. Am. Chem. Soc.* **1976**, *98*, 5055.
(19) Rio, V. C., M.S. Thesis, Kansas State University, 1979.

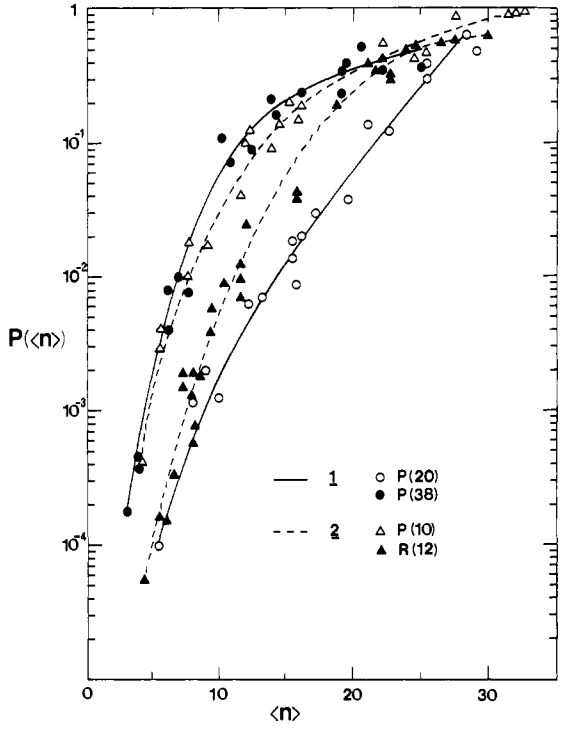

Figure 11. Reaction probability per pulse vs. average number of absorbed photons, $\langle n\rangle$, for 0.05 torr of **1** irradiated at P(20) (1046.85 cm^{-1}) and P(38) (1029.44 cm^{-1}) and 0.05 torr of **2** irradiated at P(10) (1055.63 cm^{-1}) and R(12) (1073.28 cm^{-1}). Data for **1** and **2** are illustrated with solid and dashed curves, respectively.

Table III. Summary of $P(\phi)$, ϕ, σ_L, $\langle n\rangle$, and $\langle n_r\rangle$ for Esters **1**-**4**[a]

ester	$P(\phi)$[b]	ϕ (J, cm^2)	σ_L ($\times 10^{-19}$ cm^2)	$\langle n\rangle$[c]	$\langle n_r\rangle$[d]
ethyl acetate	10^{-1}	1.5	2.8	20.2	202
ethyl fluoroacetate	10^{-1}	1.2	2.8	15.7	157
ethyl acrylate	10^{-1}	2.2	1.6	16.5	165
n-butyl acetate	10^{-1}	1.8	2.0	17.4	174
ethyl acetate	10^{-2}	0.9	3.1	13.4	1340
ethyl fluoroacetate	10^{-2}	0.8	2.8	10.5	1050
ethyl acrylate	10^{-2}	1.5	1.9	13.4	1340
n-butyl acetate	10^{-2}	1.2	2.5	14.5	1450
ethyl acetate	10^{-3}	0.6	3.3	9.5	9500
ethyl fluoroacetate	10^{-3}	0.6	2.7	7.6	7600
ethyl acrylate	10^{-3}	1.2	2.0	11.3	11300
n-butyl acetate	10^{-3}	0.9	2.7	11.7	11700

[a] Ethyl acetate: $\sigma = 3.7 \times 10^{-19}$ cm^2/molecule, 0.05 torr, ν = 1046.85 cm^{-1}. $n_{thermal} = 1.0$.[e] Ethyl fluoroacetate: $\sigma = 2.3 \times 10^{-19}$ cm^2/molecule, 0.07 torr $\nu = 1073.28$ cm^{-1}, $n_{thermal} = 1.0$.[e] Ethyl acrylate: $\sigma = 2.4 \times 10^{-19}$ cm^2/molecule, 0.05 torr, ν = 1071.88 cm^{-1}, $n_{thermal} = 1.3$.[e] *n*-Butyl acetate: $\sigma = 3.0 \times 10^{-19}$ cm^2/molecule, 0.10 torr, $\nu = 1041.28$ cm^{-1}, $n_{thermal} = 1.3$.[e] [b] Fraction of molecules within irradiated volume that react per pulse. [c] Average number of photons absorbed per molecule within irradiated volume. [d] Average number of photons absorbed per reacted molecule. [e] Thermal vibrational energy at 298 K in photons per molecule which must be added to $\langle n\rangle$ to obtain the total vibrational energy.

The $P(\phi)$ and $P(\langle n\rangle)$ data for **1** and **2** (Figures 9–11) were obtained with considerable care by three different workers and are believed to be as accurate as achievable with the available instrumentation. Although not all data are plotted, over 60 independent determinations of $P(\phi)$ vs. ϕ for **1** were obtained at five different laser frequencies (1053.9, 1050.4, 1048.7, 1046.9, and 1029.4 cm^{-1}) utilizing both long and short laser pulses at 1046.9 cm^{-1}. For **2** over 30 determinations were obtained at four laser frequencies (1078.6, 1073.3, 1070.5, and 1055.6 cm^{-1}). Similar, although less extensive data for **3**–**5** were also obtained

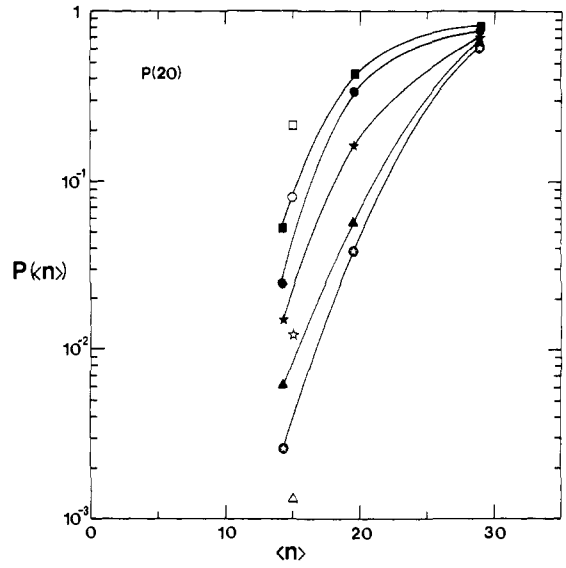

Figure 12. Reaction probability per pulse for various pressures of **1** irradiated at P(20) (1046.85 cm^{-1}): ◘, 0.05 torr; ▲, 0.10 torr; ★, 0.20 torr; ●, 0.50 torr; ■, 1.0 torr. Open symbols represent reaction probabilities of isopropyl bromide in a 95:5 ethyl acetate:isopropyl bromide mixture at various pressures: △, 0.10 torr, ☆, 0.20 torr, ○, 0.50 torr, □, 1.0 torr. Note the increase in $P(\langle n \rangle)$ at constant $\langle n \rangle$ with increasing pressure of neat **1**.

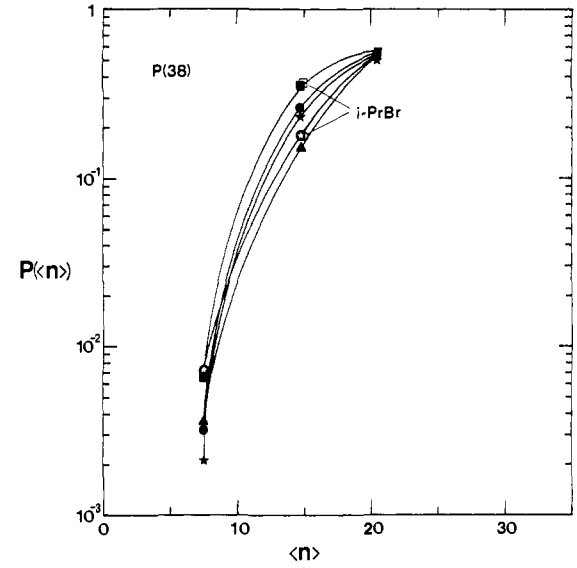

Figure 13. Same as Figure 12 except for irradiation at P(38) (1029.44 cm^{-1}).

but are not plotted here (cf. Table III). The $P(\phi)$ values are very sensitive to any experimental error in ϕ measurement because of the strong dependence of $P(\phi)$ on ϕ for $P(\phi) \lesssim 10^{-1}$; e.g., if $P(\phi) \propto \phi^4$, a ±10% error in the determination of $\phi = 1.0$ J/cm^2 would result in >twofold change in $P(\phi)$. In addition, an accurate determination of the irradiated volume is necessary. A ±10% error in measuring a 10-mm diameter laser beam would cause a ±20% error in the irradiated volume. We believe the error limits of our measurements of ϕ and the laser beam diameter are within ±10%.

D. Variation of $P(\phi)$ with Reactant Pressure. It was demonstrated in Figure 3 that the addition of a bath gas diminished significantly the yield per pulse for reaction of ethyl acetate. We interpreted these results to indicate that experiments at 0.05 torr of neat parent reactant were probably free of thermally induced reaction. Figures 12 and 13 illustrate the effect on $P(\langle n \rangle)$ of varying the pressure of neat **1** for two different laser frequencies. For 1046.9-cm^{-1} P(20) irradiation, there is a pronounced effect of reactant pressure on the reaction probability, especially at lower $\langle n \rangle$. Increasing the pressure from 0.05 to 1.0 torr results in ~20-fold increase in $P(\langle n \rangle)$ at $\langle n \rangle = 14$ and ~threefold increase at $\langle n \rangle = 25$. The open symbols at $\langle n \rangle = 15$ in Figure 12 illustrate $P(\langle n \rangle)$ for added 5% isopropyl bromide at various pressures. For a total pressure of 1.0 torr ($P(\langle n \rangle)$ for the thermal monitor is ~ two times that of ethyl acetate, illustrating an approach to intermolecular vibrational equilibration within the irradiated volume; for an equilibrated system $P(\langle n \rangle)$ for isopropyl bromide should exceed that of ethyl acetate by ~12-fold. For irradiation of **1** at 1029.4 cm^{-1} (P(38)), the effect of pressure is not nearly so pronounced and with no discernible trend; e.g., for 0.05 torr of **1**, $P(\langle n \rangle)$ is higher than for the other pressures at $\langle n \rangle = 7.5$ but lower at $\langle n \rangle = 22$. These different results reflect the extents of thermal reaction which augments the laser driven process. The explanation of the remarkable difference between the P(38) and P(20) irradiation will be given in the Discussion section.

E. Multichannel Reactants. Unlike esters **1–4**, which undergo reaction to produce a single olefinic product, *sec*-butyl acetate (**5**) and ethyl 2-bromopropionate (**6**) can react by more than one channel. The butene product distribution from **5** was independent within the experimental uncertainty of both pressure, in the range 0.05–1.0 torr, and fluence from 5 to 8 J/cm^2 (see product ratios in reaction 5). A sensitized experiment in which a mixture of 90% SiF_4 and 10% **5** at a total pressure of 0.8 torr was irradiated at 1025.29 cm^{-1} with a fluence of 0.5 J/cm^2 also produced the same product distribution. Under these conditions, nearly all the absorbed energy is deposited into SiF_4 with **5** acquiring excitation via collisional energy transfer; i.e., the entire reaction is thermally driven.

Ethyl 2-bromopropionate (**6**) can undergo reaction via the two channels shown in reaction 6. The Arrhenius parameters for these two reaction channels are not known with certainty but they should be comparable with $E_a \sim 46$–48 kcal/mol and log $A \sim 12$–13 s^{-1}. Irradiation of **6** at 1074.65 cm^{-1} and $\phi = 1.2$ J/cm^2 gave an ethylene:ethyl acrylate ratio of 3.1. For $\phi = 5.1$ J/cm^2 the ratio increased to 31. A sensitized experiment with 0.1 torr of 81% SiF_4 and 19% **6** produced a ratio of 5.1 when irradiated at 1025.29 cm^{-1} with 0.8 J/cm^2, but the ratio increased to 12.7 at $\phi = 3.3$ J/cm^2. The strong increase in product ratio at high ϕ probably is a consequence of the secondary reaction of ethyl acrylate.

Discussion

A. Thermal Monitor and Collisional Deactivation Studies. We have extended considerably our earlier studies[17] utilizing a thermal monitor molecule to probe for thermal vs. nonequilibrium laser-driven components in multiphoton reaction processes for ethyl acetate. It is necessary to test for a thermal component by adding a sufficiently small amount of thermal monitor so that changes in the sample heat capacity and quenching of the laser reaction are negligible.

Quenching by added bath gases is illustrated dramatically by Figures 3 and 4 showing that low pressures of the monitor can have a significant effect on the ethyl acetate reaction even though few monitor molecules actually acquire enough energy to react. The quenching is especially pronounced at low laser fluences. For example, at 2 J/cm^2, 0.04 torr of isopropyl bromide reduced the reaction yield from 0.02 torr of **1** by a factor of 2 ($Y_0/Y = 2.0$) although the propylene/ethylene ratio was only 0.05 (Table I). At higher fluence, more isopropyl bromide was required to produce a similar degree of quenching. For example, for a twofold decease at 3.6 J/cm^2, 0.61 torr of isopropyl bromide was required. The propylene/ethylene ratio was only 0.18; the thermal ratio would be ~270 for these conditions.

Figures 3 and 4 illustrate that isopropyl bromide was much more effective at quenching the reaction of ethyl acetate than was N_2 or He. Moreover, there was no enhancement of reaction with addition of He or N_2 as is frequently observed for laser irradiation of small molecules, which usually is attributed to collisional rotational hole filling.[20] Measurement of the reaction yield, however, is not the most sensitive way to search for collisional relaxation

(20) Jang, J. C.; Setser, D. W. *J. Phys. Chem.* **1979**, *83*, 2809.

of any bottleneck because the quenching by the added bath gas may obscure any enhanced reaction that might effect additional energy absorption. A better way is to measure directly the energy deposited in the sample vs. bath gas pressure.

The quenching trends in Figures 3 and 4 are easily rationalized. At low laser fluences, the mean ethyl acetate excitation is less than at higher fluence. The reaction rate is low for low-energy molecules and much of the reaction occurs after the laser pulse has terminated. The long mean lifetime of the low-energy molecules allows for more deactivating collisions with He, N_2, or isopropyl bromide molecules. However, few of the isopropyl bromide molecules ever achieve a sufficient level of excitation to react since the low level of excitation transcribes into a low thermal temperature.

Thermal monitoring experiments with a minimal amount of probe molecule are reported in Table II. There is a slight thermal component even at 0.05 torr of a 97:3 mixture of **1**:isopropyl bromide although the amount of monitor induced to react is virtually negligible. Increasing the pressure to 0.20 torr resulted in a 750-fold increase in reaction of isopropyl bromide at 2.49 J/cm^2, and the effect of pressure is similar to the trend noted above. Increasing the laser fluence at constant pressure (entries 1 and 2 of Table II) resulted in a greater amount of thermal reaction although the propylene/ethylene ratio did not change appreciably. The increased isopropyl bromide reaction probability reflects the increased energy input into the system, some of which is collisionally transferred to the monitor in competition with cooling processes.

Since the quenching of the thermal reaction depends on the cooling rate of the irradiated volume, there could be a dependence of the thermal component upon the geometry of the irradiated sample. Entries 1 and 4 of Table II, which differ only in the diameters of the laser beams, show a geometry effect because $P_{(i\text{-PrBr})}$ is larger for the larger diameter (19.1 mm) laser beam. The fluences were identical as shown by the similar $P_{(\text{EtOAc})}$, but $P_{(i\text{-PrBr})}$ for the smaller beam was ~25-fold less than for the larger beam. This effect can be qualitatively understood since collisions of the monitor molecules and the acetate molecules within the cylindrical-shaped irradiated volume must be in competition with various cooling processes. The latter are undoubtedly a complex interplay of diffusion, momentum transfer, conduction, etc., but a small volume will dissipate energy to the surrounding cold bath more quickly than a larger volume. The cooling processes are discussed in more detail in the accompanying paper. In general, establishing the exact thermal contribution to a reaction should be evaluated for a given irradiation geometry. Fortunately the $P_{(i\text{-PrBr})}$ are sufficiently small for both geometries at 0.05 torr that the thermal component can be ignored.

Additional results from thermal monitor experiments will be discussed below in section D.

B. Multi-Product Channels and Energy Randomization. The same isomeric butene distribution for **5** (reaction 5a–c), for direct laser irradiation and for the sensitized experiments, is evidence for energy randomization prior to reaction. The product ratios reflect the reaction path degeneracy since the Arrhenius parameters for the three reaction channels are similar.[14c] Likewise, the ethylene:ethyl acrylate product ratio of 3.1 at $\phi \leq 1.2$ J/cm^2 for **6** is in accordance with energy randomization. The rather strong dependence of the product ratio upon ϕ for reaction 6 is not expected, since the two channels have similar Arrhenius parameters. The observed increase in the ethylene:ethyl acrylate ratio to 31 at $\phi = 5.1$ J/cm^2 would be anticipated if the E_a and A factor were significantly greater[21,22] for the ethylene channel, but this does not appear probable in the present case.[23] A plausible explanation is that the ethyl acrylate that is formed during the laser pulse subsequently absorbs laser energy and reacts to form additional ethylene and acrylic acid. We have encountered a similar secondary laser-induced reaction during a single laser pulse in our investigations of ethyl 3-cyclohexenecarboxylate.[22]

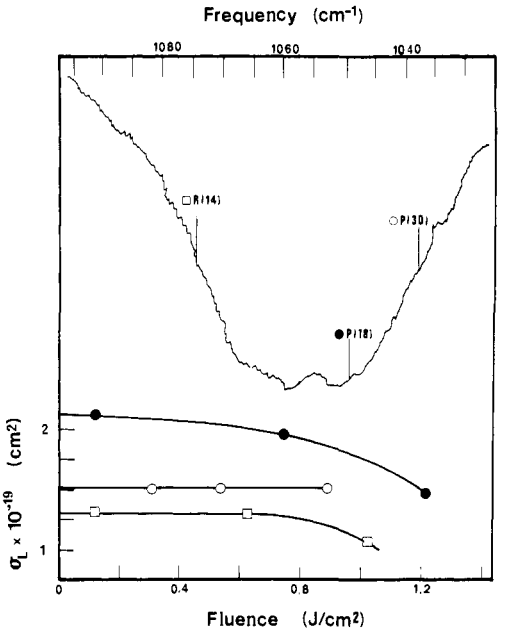

Figure 14. (Upper) Infrared spectrum of 6.0 torr of methyl acetate in 20-cm path-length cell. (Lower) Effective bulk laser absorption cross section, σ_L, vs. laser fluence for irradiation of methyl acetate at P(30) (1037.43 cm^{-1}), P(18) (1048.66 cm^{-1}), and R(14) (1074.65 cm^{-1}).

C. Absorption Measurements. Multiphoton energy absorption measurements are as fundamental as reaction probability studies. Beer's law applies to the multiphoton processes of these large molecules, and the bulk absorption cross sections, σ_L, are molecular properties independent of pressure. This is in contrast to many small molecules which exhibit collisional effects on the absorption process. The σ_L data are plotted in Figures 5–7, and σ_L, $\langle n \rangle$, and $\langle n_r \rangle$ values for $P(\phi) = 10^{-1}$, 10^{-2}, and 10^{-3} are summarized in Table III. The σ_L values are tabulated assuming that all the molecules within the irradiated volume are responsible for the ϕ/ϕ_0 ratio (eq 8). In general, the σ_L values for these large molecules are relatively insensitive to fluence. In contrast, at $\phi \sim 1$ J/cm^2 the σ_L for SF_6 is several orders of magnitude lower than the broad-band spectroscopic cross section.

The observed σ_L do have a weak dependence on ϕ which can be explained by a functional dependence of the specific level-to-level cross sections with ϕ.[12] At sufficiently high ϕ the σ_L values will always decline because of depletion of molecules by chemical reaction during the laser pulse. The onset of this trend occurs at $P(\phi) \sim 0.1$ as discussed in the following paper.[12] The σ_L extrapolate to the single-photon, broad band and cross section at low ϕ. Since the reaction probability at high ϕ reaches values between 0.5 and 1.0, nearly all molecules must be capable of absorbing the laser energy, at least at $\phi \geq 5$ J/cm^2. Therefore, the multiphoton energy absorption by an ester molecule appears to be essentially independent of the initial rotational state. This startling result is addressed in the Discussion section of the following paper.[12]

For some frequencies, σ_L increased with an increase in ϕ. Irradiation of **1** at 1029.4 cm^{-1} (Figure 5) and **2** at both 1055.6 and 1073.3 cm^{-1} (Figure 6) demonstrates such an effect. It may

(21) We have demonstrated that exit channel ratios for bifunctional reactants can be changed significantly by variations in the laser fluence if the channels have significantly different Arrhenius parameters. In essence, a reaction channel with a high Arrhenius A factor and high threshold energy can become competitive at high laser fluences.

(22) Setser, D. W.; Danen, W. C.; Nguyen, H. H. *J. Phys. Chem.*, submitted for publication.

(23) The Arrhenius parameters for **6** to our knowledge have not been reported. The E_a and A factors for related compounds such as isopropyl bromide ($E_a = 47.8$ kcal/mol; log $A = 13.6$)[14c] and ethyl acetate ($E_a = 48.0$ kcal/mol; log $A = 12.6$)[14a] are in the wrong direction. Conjugation of the double bond with the carbonyl group in the product ethyl acrylate resulting from HBr elimination from **6** would be expected to lower E_a and the A factor somewhat as compared to these model compounds.

be significant that these three frequencies all lie on the low-frequency side of the absorption band; the increase in σ_L may arise from an anharmonic red shift of the absorption band to lower frequency. We measured σ_L for methyl acetate, $CH_3CO_2CH_3$, a compound that cannot undergo the characteristic six-centered elimination (reaction 7) at 1037.43 cm^{-1} [P(30)], 1048.66 cm^{-1} [P(18)], and 1074.65 cm^{-1} [R(14)] with the results shown in Figure 14. The general decrease in σ_L with ϕ for the reactive esters does not necessarily result from product formation since a similar decrease is observed for methyl acetate. However, irradiation at 1037.43 cm^{-1}, which is on the low-frequency side of the absorption band, did not result in an increase in σ_L with ϕ as was noted for **1** and **2**. The factors influencing the dependence of σ_L on ϕ are discussed more fully in the accompanying paper.[12]

D. Reaction Probability. The $P(\phi)$ results are thought to be free of significant thermal contribution. The experimental method constrains measurements to $P(\phi) > 10^{-4}$. At low to intermediate fluences $P(\phi)$ has a high-order dependence on ϕ and $P(\phi)$ asymptotically approaches 1.0 for **3** and **5** and values between 0.5 and 1.0 for other esters. The slopes of the lines from plots of ln $P(\phi)$ vs. ln ϕ in the region $P(\phi) \sim 10^{-4} - 10^{-2}$ indicate that the reaction yield scales as ~4–6th power of ϕ. This is typical of infrared laser multiphoton induced chemical reactions. The only unusual aspect of these organic esters is that the reaction probability is very high for rather moderate fluence which allows quantitative studies for uniform fluence conditions. The possibility of extracting information from the steady-state,[24] or high ϕ, regime via ln $(1 - P(\phi))$ vs. ϕ plots is examined in the following paper.[12]

A plot of reaction probability vs. $\langle n \rangle$ is more informative than vs. ϕ since the amount of energy actually *absorbed* by molecules is more directly related to the extent of reaction.[18] The amount of energy absorbed depends upon both ϕ and σ_L; the relationship is expressed by eq 10. Figure 11 depicts $P(\langle n \rangle)$ vs. $\langle n \rangle$ for **1** and **2** at the two most extensively studied laser frequencies for each. If the reaction probability depended only upon the deposited energy, then $P(\langle n \rangle)$ would be independent of wavelength. However, *the reaction probability for the same amount of absorbed energy is frequency dependent* for both **1** and **2**. The effect is especially pronounced for **1** for which irradiation at P(38) is more effective in promoting reaction than irradiation at P(20) even for the same amount of absorbed energy. For **2** irradiation at P(10) is more effected than at R(12). Both σ_L and $P(\langle n \rangle)$ data were triple-checked, and the data unambiguously show that $P(\langle n \rangle)$ depends on frequency as well as $\langle n \rangle$ for **1** and **2**. One explanation could be slow *intramolecular* energy randomization. We reject this explanation for several reasons, one of which is the statistical nature of the two-channel reaction systems as discussed earlier. Moreover, such an explanation would appear untenable for the present results since the same absorption bands in **1** and **2** are presumably being pumped by the two different laser frequencies that give different $P(\langle n \rangle)$.

A more plausible explanation is that only a fraction of the molecules of **1** and **2** in the irradiated volume actually absorb the laser energy when irradiated at P(38) and P(10), respectively. If so, a two-component distribution of molecules is produced after laser excitation and the fraction absorbing energy will have a much higher mean energy than predicted by the $\langle n \rangle$ calculated as in Table III. The highly activated molecules have high k_E values and react more readily. The fraction that absorbs the energy probably is fluence dependent, i.e., becomes larger at higher ϕ. Experiments with SF_6,[25] OsO_4,[26] and ethyl chloride[27] have shown that many molecules remain in the low-energy levels and only a fraction (depending on ϕ) reach the quasi-continuum upon multiphoton excitation. Even though molecules as large as **1** and **2** probably do not have an anharmonicity bottleneck characteristic of small molecules, there still may be certain restrictions regarding rotational state selection in the absorption of the first photon.[12]

The ester elimination reactions are only a few kcal/mol endoergic so the deposited laser energy must be removed by bulk cooling in order to stop the thermal reaction. At the low pressures employed for this work, estimation of the minimum time for the cooling wave (see following paper[12]) suggests a time of $\lesssim$5–10 μs. For low fluence conditions, i.e., $P(\langle n \rangle) \lesssim 0.05$, most of the products are formed by postpulse processes occurring prior to the cooling wave. Only for $P(\langle n \rangle) \gtrsim 0.2$ does most of the reaction occur during the laser pulse; for $0.05 < P(\langle n \rangle) < 0.2$, both reaction during and after the laser pulse contribute to the yield.[12]

Some experiments with ethyl acetate were done to specifically test the dependence of $P(\langle n \rangle)$ on reagent pressure. Figures 12 and 13 illustrate that increasing the pressure of neat **1** at constant $\langle n \rangle$ resulted in a significantly enhanced yield per pulse for irradiation at P(20), but the effect for P(38) was less pronounced with no obvious trend. The total observed reaction yield is the sum of $P(\langle n \rangle)_{laser}$ and $P(\langle n \rangle)_{thermal}$. The $P(\langle n \rangle)_{laser}$ reflects reaction during the laser pulse and before intermolecular vibrational equilibration has occurred. For the reactant pressures utilized herein, $P(\langle n \rangle)_{thermal}$ is considered to arise almost exclusively from postpulse processes although partial equilibration may onset during the pulse at pressures $\gtrsim$0.5 torr. For a given $\langle n \rangle$ and given pressure the $P(\langle n \rangle)_{thermal}$ should be approximately constant (ignoring possible effects of multicomponent distributions). The difference in the pressure dependence of $P(\langle n \rangle)$ for P(20) and P(38) irradiation is largely explained by the much lower $P(\langle n \rangle)_{laser}$ for P(20). For example, consider $\langle n \rangle = 15$. The $P(\langle n \rangle)_{laser}$ is $\sim 4 \times 10^{-3}$ (which is the result for the lowest pressure experiments). Increasing the pressure to 1 torr gives $P(\langle n \rangle) \sim 0.10$, which must be largely of thermal origin. Thus, we can take $P(\langle n = 15 \rangle)_{thermal}$ as ~0.1. For P(38) irradiation $P(\langle n = 15 \rangle)_{laser} \sim 0.15$ and the addition of the $P(\langle n = 15 \rangle)_{thermal}$ contribution should roughly double the observed reaction probability, which indeed is the experimental result. For higher $\langle n \rangle$ the laser contribution from P(20) irradiation increases and the relative contribution of $P(\langle n \rangle)_{thermal}$ is somewhat smaller. An attempt was made to place the results on a somewhat more quantitative basis by comparing the reaction probabilities of ethyl acetate and isopropyl bromide (open symbols in Figures 12 and 13). The above argument for the P(20) experiments at 1.0 torr suggested that most of the reaction probability at $\langle n \rangle = 15$ was of thermal origin. From the most naive point of view $P(\langle n \rangle)_{i\text{-PrBr}}/P(\langle n \rangle)_{acetate}$ should be ~11, the thermal rate constant ratio. However, the ratio, in fact, is only ~3 at 1 torr and $\langle n \rangle = 15$. Thus, the pressure enhanced reaction yield of ethyl acetate is not totally thermal in the sense that both ethyl acetate and isopropyl bromide molecules are at the same temperature. This is not unexpected at a pressure of only 1.0 torr, but it makes detailed interpretation of the pressure enhancement extremely difficult. The enhancement results from two general tendencies which reinforce each other: (i) the higher pressure promotes intermolecular collisional transfer of energy and (ii) the higher pressure lengthens the time before the onset of the cooling wave. Thus, the thermal time regime begins more quickly after the pulse and lasts for a longer time as the reagent pressure is increased.

The average numbers of photons absorbed per reacted molecule, $\langle n_r \rangle$, are shown in Figure 8 for the low-pressure data; $\langle n_r \rangle \sim 16$ corresponds to the 48 kcal mol^{-1} threshold energy. The $\langle n_r \rangle$ values are qualitatively the same for all the esters. At low fluences $\langle n_r \rangle$ are large, indicating relatively inefficient utilization of laser photons; i.e., $\langle n_r \rangle \sim 1000$ for $P(\phi) = 0.01$. Since <10% of the laser radiation is actually absorbed by the sample in these experiments, only one molecule actually reacts for several thousand laser photons. Of course, these experiments were not designed to produce optimum $\langle n_r \rangle$ values. The photon efficiency increases considerably at higher $P(\phi)$; e.g., $\langle n_r \rangle \sim 100$ at $P(\phi)$, ~ 0.1. At $P(\phi) \sim 1.0$, the $\langle n_r \rangle$ values approach the mean energy associated with the steady-state reaction rate, which is shown to be ~20 in the following paper. Thus, the deposited energy is most efficiently utilized for high fractional reactions. Our $\langle n_r \rangle$ values pertain only to laser-driven reaction. With increased pressures the deposited

(24) Quack, M. *J. Chem. Phys.* **1978**, *69*, 1282.
(25) Sudbo, Aa. S.; Schulz, P. A.; Kraynovich, D. J.; Lee, Y. T.; Shen, Y. R. *Opt. Lett.* **1979**, *4*, 219.
(26) Ambartzumian, R. V.; Makarov, G. N.; Puretzky, A. A. *Opt. Commun.* **1978**, *27*, 79.
(27) Dai, H.-L.; Kung, A. H.; Moore, C. B. *J. Chem. Phys.* **1980**, *73*, 6124.

energy could be utilized to drive a thermal reaction which would raise the yield. The photon utilization efficiency could certainly be improved quite dramatically by judicious choice of laser frequency, using high laser fluences, long reaction cells, multiple reflection optics, etc.

The fact that $\langle n_r \rangle$ are comparable for the small and large ester molecules suggests that the laser energy is being more efficiently utilized by the larger molecules. This could be for two reasons: (1) smaller fraction of molecules absorbing the laser energy and (2) greater contribution of post-pulse reaction. We favor the first possibility.

Summary and Conclusions

(1) Extensive data, obtained under carefully controlled conditions, for infrared multiphoton absorption and reaction probabilities have been collected for a series of organic esters. The data for ethyl acetate and ethyl fluoroacetate are believed to be especially reliable and form the basis for detailed modeling studies reported in the accompanying paper.[12]

(2) The extent of collisional energy transfer from excited ester molecules to cold molecules was characterized by adding a small percent of a "thermal monitor". Experiments with a 97:3 ethyl acetate/isopropyl bromide mixture indicated that the reaction probability of isopropyl bromide was much smaller than the reaction probability of ethyl acetate providing the pressure was <0.10 torr. Above 0.10 torr, an increasingly significant fraction of reaction occurred as a consequence of intermolecular energy transfer.

(3) Addition of bath gas reduced the reaction probability significantly, especially at low fluence. Large molecules were more effective deactivators than di- or monoatomic gases, which indicated that the bath gas was causing deactivation of highly vibrationally excited molecules similar to results from chemical activation studies.

(4) Direct and sensitized excitation of *sec*-butyl acetate gave the same product distribution which was independent of ester pressure and laser fluence. Direct and sensitized excitation of ethyl 2-bromopropionate gave similar results, indicating that vibrational energy randomization precedes chemical reaction for direct excitation.

(5) Bulk laser absorption cross sections, σ_L, vs. ϕ, were measured for six esters. The cross sections were independent of pressure but were mildly dependent on fluence. At low fluence, ~0.1 J cm^{-2}, the laser cross section had the same value as the broad-band cross section at the same frequency.

(6) A plot of log $P(\phi)$ vs. log ϕ showed approximately linear behavior for $P(\phi)$ values of 10^{-2} to 10^{-4} with slopes of 4–6 reflecting the strong dependence of the reaction probability on fluence. At fluences $\gtrsim$4 J/cm^2 the $P(\phi)$ curve asymptotically approached constant values, usually between 0.5 and 1.0.

(7) Plots of $P(\langle n \rangle)$ vs. the average number of absorbed photons, $\langle n \rangle$, for ethyl acetate and ethyl fluoroacetate demonstrated that *the reaction probability for the same amount of absorbed energy was dependent on laser frequency*. This was interpreted as showing that only a certain fraction of molecules, rather than all molecules within the irradiated volume, absorb the laser energy to produce a two- (or greater) component energy distribution. This fraction probably is fluence dependent. The situation may occur for the other molecules too, even though it was definitely shown only for ethyl acetate and ethyl fluoroacetate.

(8) The reaction probability of ethyl acetate irradiated at P(20) was very dependent on pressure for constant $\langle n \rangle$, indicating an enhancement of yield because of thermal contributions at higher pressures. For excitation with P(38) the pressure effect for constant $\langle n \rangle$ was less significant because the laser-driven component was much larger than for P(20) experiments.

Acknowledgment is made to the National Science Foundation (Grant CHE77-22645 and, in part, 77-21380) for support of this work and to H. H. Nguyen and J. C. Jang for rechecking several of the experimental data.

Registry No. 1, 141-78-6; 2, 459-72-3; 3, 105-38-4; 4, 123-86-4; 5, 105-46-4; 6, 535-11-5.

Multiphoton Laser-Induced Chemistry of Organic Esters: Comparison with Master Equation Calculated Results

J. C. Jang, D. W. Setser, and Wayne C. Danen*

Contribution from the Department of Chemistry, Kansas State University, Manhattan, Kansas 66506. *Received April 16, 1981*

Abstract: A master equation formulation without bottlenecks has been used to examine some general and specific features of the CO_2 laser-induced unimolecular reactions of organic esters (experimental studies are presented in the preceding paper). The general features should apply to other large molecules having a reaction threshold near 45 kcal mol^{-1} and comparable absorption cross section. The incubation period and postpulse phenomena that are (or can be) very important in bulb experiments for large molecules are illustrated by calculation. For exoergic or mildly endoergic reactions a postpulse bulk cooling wave is important for limiting the extent of reaction. The specific features include assignment of level-to-level absorption cross sections and comparison of experimental and calculated reaction probabilities for ethyl acetate and ethyl fluoroacetate excited at two different wavelengths. The calculations, which include postpulse collisions, reproduce the general trends in the data. Nearly quantitative agreement is obtained in the steady-state (high fluence) regime. The calculations generally underestimate the reaction probability at low fluence, and the discrepancy is especially serious for ethyl acetate and ethyl fluoroacetate at the P_{38} and P_{10} frequencies, respectively. These deficiencies can be rationalized by assuming that only a certain fluence-dependent fraction of the molecules participate in multiphoton absorption. Experimental data and calculated results also are given for excitation of ethyl fluoroacetate in He and CF_4 buffer gas.

I. Introduction

The preceding paper[1] reported the reaction probabilities of organic esters for a given absorbed CO_2 laser energy. In the present paper, master equation computations are done to provide insight into the physical and chemical processes resulting from CO_2 laser irradiation of the organic esters. The experimental constraints to the model are the reaction probabilities and the absorbed laser energy for a wide range of laser fluences. The master equation was formulated assuming that (i) the ester molecules are in the quasi-continuum region, even at room temperature, (ii) RRKM unimolecular rate constants describe the

(1) Danen, W. C.; Rio, V.; Setser, D. W. *J. Am. Chem. Soc.*, preceding paper in this issue.

0002-7863/82/1504-5440$01.25/0 © 1982 American Chemical Society